

between the wing bending vibration and the short period oscillation of the aircraft.

Acknowledgment

The author is grateful to Ken Griffin at Cranfield Institute of Technology for many useful discussions. He also wishes to thank his wife, Mala, for sustained encouragement.

References

¹Banerjee, J. R., "Flutter Characteristics of High Aspect Ratio Tailless Aircraft," *Journal of Aircraft*, Vol. 21, Sept. 1984, pp. 733-736.

²Theodorsen, T., "General Theory of Aerodynamic Instability and Mechanisms of Flutter," NACA TR- 496, 1934.

Spanwise Displacement of a Line Vortex Above a Wing – A Simple Calculation Scheme

Yunggui Jung* and Donald D. Seath†

University of Texas at Arlington, Arlington, Texas

I. Introduction

WHEN a wing encounters a concentrated tip vortex, its aerodynamic characteristics are substantially altered due to nonlinear interaction. While the vortex affects the wing loads, the wing in turn affects the vortex path through its vorticity field.

Hancock¹ noticed the displacement of a streamwise line vortex over a two-dimensional wing and gave analytic expression for the sidewash velocity induced on the vortex by the wing trailing vorticity. Experimental evidence of this type of vortex motion was reported by Patel and Hancock² in their flow visualization study. Vortex motion due to secondary separation was observed by Harvey and Perry³ in their investigation of trailing vortices in the vicinity of the ground. Recently, the displacement of a tip vortex above a two-dimensional wing surface was carefully measured in a low-speed wind tunnel for various conditions by Seath and Wilson.⁴

Meanwhile, it was recognized on the computational side^{5,6} that the originally straight vortex should be allowed to align itself with the local streamline direction in order to obtain a better solution to the vortex-wing interaction calculations.

It is generally believed that some kind of iteration scheme is necessary to account for the mutual influence between the vortex and the wing trailing vorticity and, thus, to obtain an acceptable vortex path and its effect on induced airloads. However, for the flow conditions considered in this paper, i.e., low subsonic speed, it is found that the detailed temporal variation of the wing trailing vortex sheet due to the deforming line vortex has little effect on the motion of the vortex line over the wing surface, and that the spanwise displacement of a line vortex can be calculated in a straightforward manner without iteration coupled with wake evolution.

The present method is based on the lifting line solution of the spanwise load distribution. A single lifting line cannot adequately represent a wing as far as the chordwise variation of the wing vorticity is concerned. However, a very simple trick of redistributing the calculated bound vorticity along the chord in accordance with the "thin airfoil theory" produces surprisingly good results.

II. Description of the Present Method

The model consists of an infinite line vortex, which is originally parallel to the freestream, and a finite wing as shown in Fig. 1, together with the coordinate system.

Received Oct. 22, 1986; revision received Nov. 23, 1987. Copyright © American Institute of Aeronautics and Astronautics, Inc., 1987. All rights reserved.

*Graduate Teaching Assistant, Department of Aerospace Engineering.

†Professor, Department of Aerospace Engineering.

The velocity field induced by an infinite line vortex is given by the Biot-Savart law as

$$V_i(r) = \frac{\Gamma_o \times r}{2\pi r^2} \quad (1)$$

where V_i is the induced velocity, Γ_o the circulation of the line vortex, and r the radial vector from the vortex line to a field point. The induced angle of attack at any section along the span is obtained by taking the z -component of this induced velocity and dividing it by the freestream velocity. Thus for a vortex of height h

$$\alpha_i(y) = \frac{\Gamma_o}{2\pi V_\infty} \frac{y}{h^2 + y^2} \quad (2)$$

where α_i is the induced angle of attack, and V_∞ the freestream velocity. If we regard this induced angle of attack as additional twist to the section angle of attack of the wing in a uniform freestream, we can calculate the spanwise variation of circulation by solving a modified lifting line equation⁷

$$\Gamma(y) = \frac{1}{2} a_o(y) c(y) V_\infty \left[(\alpha_w + \alpha_i) - \frac{1}{4\pi V_\infty} \int_{-b/2}^{b/2} \frac{d\Gamma}{dy}(\eta) \frac{d\eta}{y - \eta} \right] \quad (3)$$

Approximate solution to this equation can be obtained to any desired accuracy by a suitable iteration scheme combined with a numerical quadrature, e.g., Ref. 8.

Whereas $\Gamma(y)$ is usually associated with a lifting line located at the quarter-chord line of the wing, we can distribute the total circulation at any section along the chord so that we have as many lifting lines as we want. From the thin airfoil theory we know for a flat plate at an angle of attack α

$$\gamma(\theta) = 2V_\infty \alpha \tan(\theta/2) \quad (4)$$

where γ is the vortex strength and θ is related to x by

$$x = (c/2)(1 + \cos\theta)$$

If we have n sublifting lines to represent the airfoil chord, the strength of each line may be obtained by integrating Eq. (4). This gives

$$\Gamma_i = \frac{\Gamma}{\pi} [\theta - \sin\theta] \frac{\theta_i}{\theta_{i-1}} \quad i = 1, 2, \dots, n \quad (5)$$

where n is the total number of lifting lines along the chord.

Each of these lifting lines sheds a vortex sheet of strength $-d\Gamma_i/dy$ downstream. For simplicity, we may assume that all the vortex sheets remain undistorted and parallel to the freestream. Therefore, if the wing is at 0 deg incidence, all the vortex sheets will be in the $x = y$ plane. Then, the sidewash

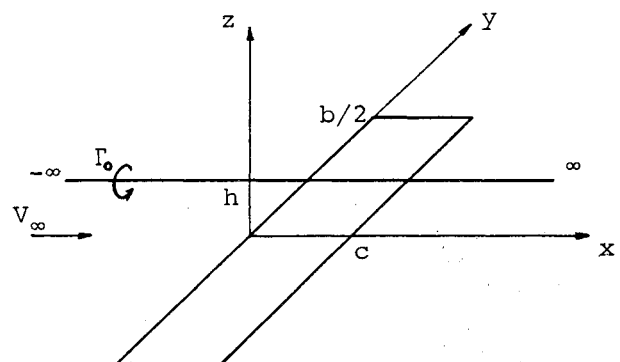


Fig. 1 Model and coordinate system.

velocity induced at a point on the vortex line by the i th trailing vortex sheet is

$$v_i(x, y, h) = \frac{h}{4\pi} \left(1 + \frac{|x - x_i|}{\sqrt{(x - x_i)^2 + h^2}} \right) \int_{-b/2}^{b/2} \frac{d\Gamma}{dy}(\eta) \frac{d\eta}{h^2 + (\eta - y)^2} \quad (6)$$

and the total sidewash at the same point is

$$v(x, y, h) = \sum_{i=1}^n v_i(x, y, h) \quad (7)$$

From this we can calculate the spanwise displacement of the vortex by time integration.

Convergence of the calculations is expected on the grounds that the influence of the vortex sheets on fluid particles located far upstream of the wing is negligible. Thus, some part of the free vortex does not move sideways.

As the vortex line deforms from its initial straight line, the induced airload will change accordingly. However, unless the free vortex is very close to the wing surface, we may further assume that this change is small for most of the wing. Then, we may freeze the trailing vortex sheets at the initial state. This means that we only need to compute the trailing vorticity due to the free vortex once and for all and do not have to update the wake field each time the free vortex assumes a new position. It turns out that this assumption is totally adequate for the test cases considered in the present paper.

III. Application and Discussion

The present method has been applied to a low subsonic vortex-airfoil interaction problem with very encouraging results. The input data were taken from the wind tunnel tests conducted at the University of Texas at Arlington by Seath and Wilson.⁴ The test setup is shown in Fig. 2.

Specifically, the vortex strength $\Gamma_0/V_\infty c = 0.288$; wing span $b = 3$ ft; lift curve slope $a_0 = 6.0/\text{rad}$; chord length $c = 10$ in.; vortex heights $h/c = 0.075, 0.095$, and 0.13 . With these values, induced angles of attack were obtained, and the modified lifting line equation was solved via the numerical iteration scheme of Multhopp using 81 spanwise stations. The resulting circulation was then distributed along the chord into 10 subsplitting lines located at $x/c = 0.05, 0.15, \dots, 0.95$.

The results are shown in Figs. 3-5. As seen in these figures the agreement with the experimental data is quite striking when we recall that the wake of the wing was "frozen" at its initial state with no later update. Figure 6 shows vortex

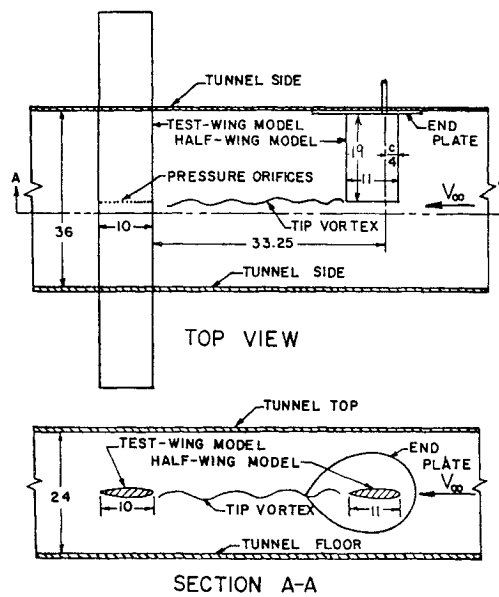


Fig. 2 Test setup.⁴

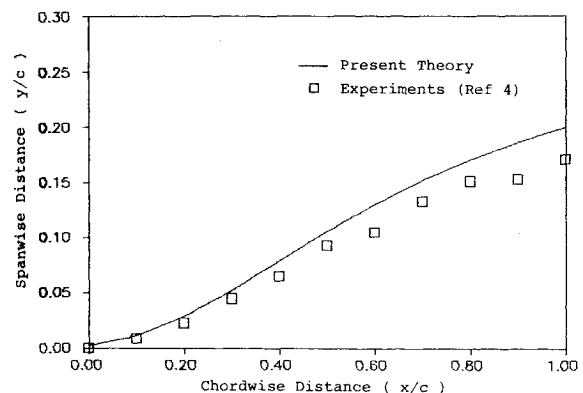


Fig. 3 Vortex path ($h/c = 7.5\%$, $\Gamma_0/V_\infty c = 0.288$).

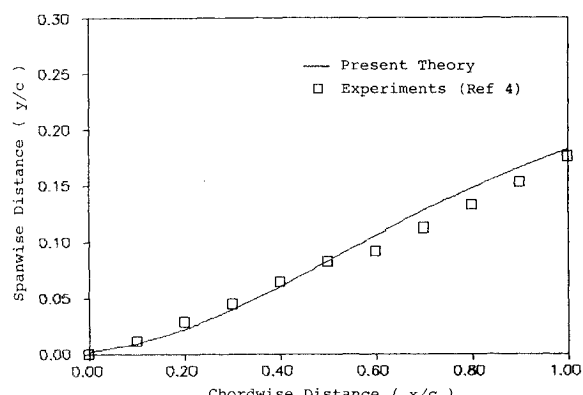


Fig. 4 Vortex path ($h/c = 9.5\%$, $\Gamma_0/V_\infty c = 0.288$).

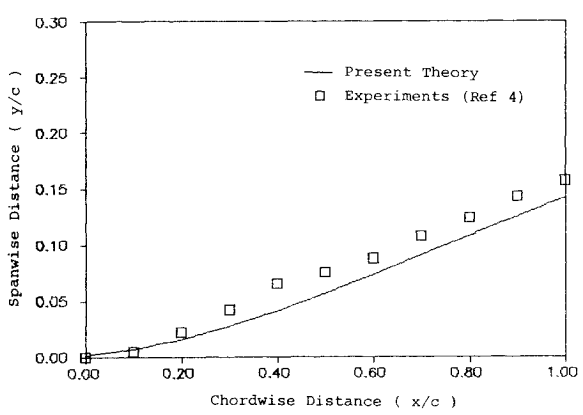


Fig. 5 Vortex path ($h/c = 13\%$, $\Gamma_0/V_\infty c = 0.288$).

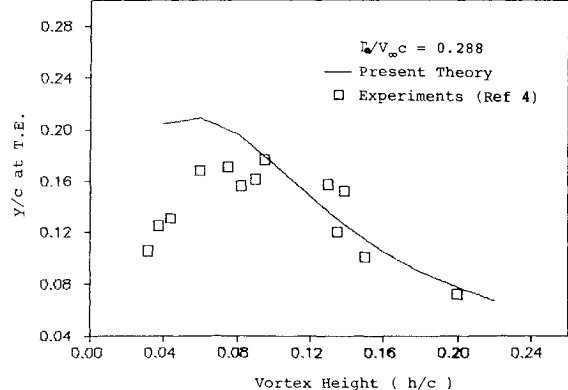


Fig. 6 Spanwise displacement vs height of vortex.

displacement at the wing trailing edge for various vortex heights. Here again, the present theory produces reasonable estimates. As is anticipated, however, a potential vortex model overpredicts the vortex effect in a very close encounter of vortex and wing due to its singularity at the center. This is evident in the figure by the deviation of the curve from the squares for h/c less than about 0.1. This situation may be improved by modeling a finite vortex core.

Overall, the results are very encouraging, and this suggests that the present method may be used as a preprocessor to prescribe the vortex path over a lifting surface for vortex-lifting surface interaction calculations within the restrictions of the potential flow assumptions. This will eliminate the need to assume a straight vortex and update the whole flow field as well as the vortex path. Or, in cases where complex configurations are involved, the present method may provide a reasonable starting position of the vortex for a coupled iteration scheme.

Acknowledgment

A portion of the work was performed under Army Research Office Contract DAAG 29-84-K-0131, Experimental Simulation of Transonic Vortex-Airfoil Interactions.

References

- ¹Hancock, G. J., "Aerodynamic Loading Induced on a Two-Dimensional Wing by a Free Vortex in Incompressible Flow," *The Aeronautical Journal of the Royal Aeronautical Society*, Vol. 75, June 1971, pp. 413-416.
- ²Patel, M. H. and Hancock, G. J., "Some Experimental Results of the Effect of a Streamwise Vortex on a Two-Dimensional Wing," *Aeronautical Journal*, April 1974, pp. 151-155.
- ³Harvey, J. K. and Perry, F. J., "Flowfield Produced by Trailing Vortices in the Vicinity of the Ground," *AIAA Journal*, Vol. 9, Aug. 1971, pp. 1659-1660.
- ⁴Seath D. D. and Wilson, D. R., "Vortex-Airfoil Interaction Tests," *AIAA Paper 86-0354*, Jan. 1986.
- ⁵Maskew, B., "Predicting Aerodynamic Characteristics of Vortical Flows on Three-Dimensional Configurations Using a Surface-Singularity Panel Method," AGARD-CP-342, 1983.
- ⁶Steinhoff, J., Ramachandran, K., and Suryanarayanan, K., "The Treatment of Convected Vortices in Compressible Potential Flow," AGARD-CP-342, April 1983.
- ⁷Karamcheti, K., *Principles of Ideal-Fluid Aerodynamics*, John Wiley, New York, 1966, Chap. 19, pp. 538-545.
- ⁸Bisplinghoff, R. L., Ashley, H., and Halfman, R. L., *Aeroelasticity*, Addison-Wesley, Reading, Mass., 1955, Chap. 5, pp. 231-237.

Divergence Study of a High-Aspect-Ratio, Forward Swept Wing

Stanley R. Cole*

NASA Langley Research Center, Hampton, Virginia

Introduction

THE present study was conducted to obtain data that could be used to assess the prediction capabilities of a currently available aeroelastic code for a high-aspect-ratio, forward-swept wing. A wind tunnel experiment was conducted in the NASA Langley Transonic Dynamics Tunnel (TDT) on a model with a panel aspect ratio of 9.16 (unswept). Aeroelastic analyses were conducted for each condition tested in the TDT

Presented as Paper 86-0009 at the AIAA 24th Aerospace Sciences Meeting, Reno, NV, Jan. 6-9, 1986; received Feb. 2, 1986; revision received Nov. 23, 1987. Copyright © 1986 American Institute of Aeronautics and Astronautics, Inc. No copyright is asserted in the United States under Title 17, U.S. Code. The U.S. Government has a royalty-free license to exercise all rights under the copyright claimed herein for Governmental purposes. All other rights are reserved by the copyright owner.

*Aerospace Technologist, Configuration Aeroelasticity Branch. Senior Member AIAA.

for this comparison. The wind tunnel model was tested at various forward sweep angles. A rectangular tip shape was used during most of the experiment. A tip parallel to the flow in the 45 deg forward-sweep position was also tested for further correlation with analysis. General aeroelastic characteristics of the high-aspect-ratio, highly swept wing, and the prediction capabilities of the analysis code are discussed in this Note.

Test Apparatus and Procedures

The model used in this study was untapered, had a 4.51 ft semispan and a semispan aspect ratio of 9.16 in the unswept position. The airfoil section was a NACA 0014. The model wing was constructed of a layered fiberglass shell, which provided both structural stiffness and the airfoil shape, with a rectangular aluminum spar located at the 30% chord position to increase the bending stiffness. Semicircular wing tips made of balsa wood were used to improve the flow over what would otherwise have been a blunt wing tip in the forward-sweep positions. The model was clamped in a cantilevered manner to the wind-tunnel sidewall.

The model was positioned manually to sweep angles Λ of 0, -15, -30, -45 and -60 deg. A composite photograph showing the model in the various sweep angles is shown in Fig. 1. The model was tested with a rectangular wing tip at each azimuth angle as shown in the figure. In addition, the wing tip was modified such that the tip was parallel to the freestream flow when tested in the $\Lambda = -45$ deg position. The two tip shapes are shown in Fig. 1 at $\Lambda = -45$ deg.

Experimental predictions of static aeroelastic divergence were made using subcritical response techniques.¹ For each sweep angle tested, subcritical data were taken at gradually increasing values of dynamic pressure. At each dynamic pressure q , the model angle of attack was first adjusted to a 1-g lift condition so that the weight of the model was aerodynamically supported. The angle of attack was then incrementally increased and the root bending moment M_e was measured at each angle of attack α . Typical data obtained for the subcritical response divergence predictions are shown in Fig. 2. These data were used to predict the dynamic pressure at which divergence would occur. Two subcritical response techniques, an improved static Southwell method and the divergence index method, were used during this test. Reference 1 discusses these prediction methods in greater detail.

Analytical Tools

Aeroelastic analyses were conducted for the wind-tunnel model to determine the validity of the analysis code for a high-aspect-ratio, highly swept wing. A vibration analysis was performed with the finite-element method program² Engineering Analysis Language (EAL). General beam elements were utilized to assemble the finite-element model. Elements were ar-

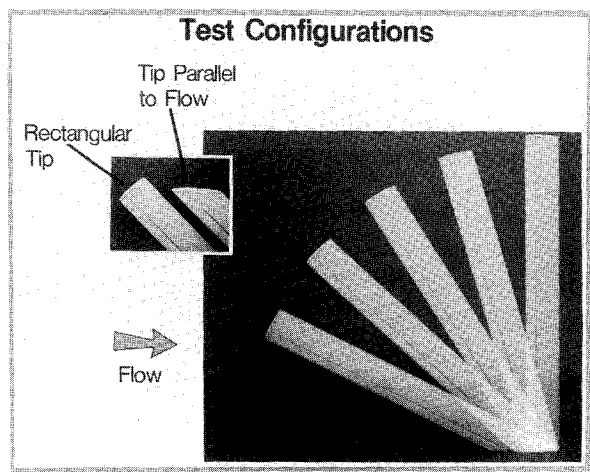


Fig. 1. Composite photograph showing each sweep angle tested and the two tip shapes tested in the $\Lambda = -45$ deg configuration.